



Earth-Moon Lyapunov to Lyapunov Mission: Long Time Duration, Low-Thrust Transfer

Maxime Chupin, Thomas Haberkorn, Emmanuel Trélat

► To cite this version:

Maxime Chupin, Thomas Haberkorn, Emmanuel Trélat. Earth-Moon Lyapunov to Lyapunov Mission: Long Time Duration, Low-Thrust Transfer. 2015. hal-01223738v1

HAL Id: hal-01223738

<https://inria.hal.science/hal-01223738v1>

Preprint submitted on 6 Nov 2015 (v1), last revised 30 Jun 2016 (v2)

HAL is a multi-disciplinary open access archive for the deposit and dissemination of scientific research documents, whether they are published or not. The documents may come from teaching and research institutions in France or abroad, or from public or private research centers.

L'archive ouverte pluridisciplinaire **HAL**, est destinée au dépôt et à la diffusion de documents scientifiques de niveau recherche, publiés ou non, émanant des établissements d'enseignement et de recherche français ou étrangers, des laboratoires publics ou privés.

EARTH-MOON LYAPUNOV TO LYAPUNOV MISSION: LONG TIME DURATION, LOW-THRUST TRANSFER *

MAXIME CHUPIN¹, THOMAS HABERKORN² AND EMMANUEL TRÉLAT³

Abstract. In this work, we develop a new method to design missions with low-thrust propulsion. In the Circular Restricted Three Body Problem, the knowledge of invariant manifolds helps us to initialize an indirect method solving a transfer mission between periodic Lyapunov orbits. Indeed, using the Pontryagin Maximum Principle, the optimal control problem is solved using Newton-like algorithms finding the zero of a shooting function. We first compute an admissible trajectory using a heteroclinic orbit between the two periodic orbits. It is then used to initialize a multiple shooting method in order to release the constraint. We finally optimize the terminal points on the periodic orbits. Moreover, we use continuation methods on position and on thrust, in order to gain robustness.

Résumé. Dans ce travail, on développe une nouvelle méthode pour construire des missions à faible poussée. Dans le problème restreint des trois corps, la connaissance des variétés invariantes nous permet d'initialiser une méthode indirecte utilisée pour calculer un transfert entre orbites périodiques de Lyapunov. En effet, par l'application du Principe du Maximum de Pontryagin, on obtient la commande optimale par le calcul du zéro d'une fonction de tir, trouvé par un algorithme de Newton. Dans un premier temps, on construit une trajectoire admissible en passant par une trajectoire hétérocline reliant les deux orbites périodiques. Celle-ci est alors utilisée pour initialiser un tir multiple nous permettant de relâcher la contrainte de rejoindre la trajectoire hétérocline. Enfin, on optimise la position des points de départ et d'arrivée sur les orbites périodiques. De plus, pour rendre nos méthodes plus robustes, on utilise des méthodes de continuation sur la position et sur la poussée.

2010 Mathematics Subject Classification. 49M05, 70F07, 49M15.

Received: date / Accepted: date.

1. INTRODUCTION

Since the late '70s, study of libration point orbits has been of great interest. Indeed, several missions such as ISEE-3 (NASA) in 1978, SOHO (ESA-NASA) in 1996, GENESIS (NASA) in 2001, PLANK (ESA) in 2007 etc. have put this design knowledge into practice. A more profound understanding of the available mission options has also emerged due to the theoretical, analytical, and numerical advances in many aspects of libration point mission design.

Keywords and phrases: Three Body Problem, Optimal Control, Low-Thrust Transfer, Lyapunov Orbit, Continuation Method

* *This work is dedicated to Philippe Augros.*

¹ LJLL-UPMC – Paris, Airbus Defence and Space – Les Mureaux, e-mail: chupin@ljl1.math.upmc.fr

² MAPMO – Orléans, e-mail: thomas.haberkorn@univ-orleans.fr

³ LJLL-UPMC – Paris, e-mail: emmanuel.trelat@upmc.fr

There exists a huge number of references on the problem of determining low-cost trajectories by using the properties of Lagrange points. For instance, the authors in [13, 18, 30] have developed very efficient methods to find “zero cost” trajectories between libration point orbits. They used dynamical system methods to construct heteroclinic orbits from invariant manifolds between libration point orbits and managed to get infinite time uncontrolled transfers. These orbits have been used with impulse engines of spacecrafts to construct finite time transfers. In this work, we want to perform the transfer with a low-thrust propulsion, so impulses to reach heteroclinic orbits are prohibited.

Manifolds has been used in low-thrust mission in [21, 22]. The low-thrust propulsion is introduced by means of special attainable sets that are used in conjunction with invariant manifolds to define a first-guess solution. Then, they optimize their solution using an optimal control formalism.

In [8], the author recently developed a very efficient method to compute an optimal low-thrust transfer trajectory in *finite* time without using invariant manifolds of the three body problem. It is based on a three-step solution method using indirect methods and continuations methods and it gives good results.

To compute the required transfer with a low thrust we will use indirect methods coming from the Pontryagin Maximum Principle [23]. Initialization of indirect methods with dynamics properties is a real challenge in order to improve the efficiency of indirect methods (see [27] and references therein). Indeed the main difficulties of such methods is to initialize the Newton-like algorithm, and the understanding of the dynamics can be very useful to construct an admissible trajectory for the initialization. Moreover, continuation methods as used in [12] or [6] are crucial to give robustness to these indirect methods. The aim of this paper is to combine all these mathematical aspects of dynamics, optimal control and continuation methods to design low-thrust transfer between libration point orbits.

First, in Section 2, we introduce the mission we want to perform and compute. We introduce the paradigm of the Circular Restricted Three Body Problem and we state our optimal control problem.

Then, in Section 3 we recall dynamical properties of the circular restricted three body problem, such as equilibrium points, Lyapunov periodic orbits, and invariant manifolds. We present the mathematical tools used to numerically compute the periodic orbits and the manifolds. In particular, we introduce in this part the continuation method which we will use throughout this article.

Then, in Section 4, we develop our method with an example mission. We first compute a heteroclinic orbit between the two Lyapunov periodic orbits. Then, fixing the departure point near L_1 and the arrival point near L_2 and with a not too small thrust (60 N), we perform two small transfers from the Lyapunov orbit around L_1 to the heteroclinic one, and from the heteroclinic orbit to the Lyapunov orbit around L_2 . Then, thanks to a multiple shooting method we release the constraint on the position of the matching points on the heteroclinic orbit and decrease the thrust to the targeted one (0.3 N). Finally, we optimize departure and the arrival points on the periodic orbits to satisfy the necessary transversality conditions given by the Pontryagin Maximum Principle.

Finally in section 5 we present another mission with a heteroclinic orbit with two revolutions around the Moon.

2. THE MISSION

First, let us introduce the model of the problem.

2.1. Circular Restricted Three Body Problem (CRTBP)

We use the paradigm of the Circular Restricted Three Body Problem. In this section we will follow the description by [17].

Let us consider a spacecraft in the field of attraction of Earth and Moon. We consider an inertial frame \mathcal{I} in which the vector differential equation for the spacecraft’s motion is written as:

$$m \frac{d\mathbf{R}}{dt} = -GM_1 m \frac{\mathbf{R}_{13}}{R_{13}^3} - GM_2 m \frac{\mathbf{R}_{23}}{R_{23}^3} \quad (1)$$

where M_1 , M_2 and m are the masses respectively of Earth, the Moon and the spacecraft, \underline{R} is the satellite vector position, \underline{R}_{13} is the vector Earth-satellite and \underline{R}_{23} is the vector Moon-satellite. G is the gravitational constant. Let us describe the simplified general framework we will use.

Problem Description. To simplify the problem, and use a general framework, we consider the motion of the spacecraft P of negligible mass moving under the gravitational influence of the two masses M_1 and M_2 , referred to as the primary masses, or simply the *primaries* (here Earth and Moon). We denote these primaries by P_1 and P_2 . We assume that the primaries have circular orbits around their common center of mass. The particle P is free to move all around the primaries but cannot affect their motion.

The system is made adimensional by the following choice of units: the unit of mass is taken to be $M_1 + M_2$; the unit of length is chosen to be the constant distance between P_1 and P_2 ; the unit of time is chosen such that the orbital period of P_1 and P_2 about their center of mass is 2π . The universal constant of gravitation then becomes $G = 1$. The conversion from units of distance, velocity and time in the unprimed, normalized system to the primed, dimensionalized system is

$$\begin{aligned} \text{distance} \quad d' &= l_* d, \\ \text{velocity} \quad s' &= v_* s, \\ \text{time} \quad t' &= \frac{t_*}{2\pi} t, \end{aligned} \tag{2}$$

where we denote by l_* the distance between P_1 and P_2 , v_* the orbital velocity of P_1 and t_* the orbital period of P_1 and P_2 .

We define the only parameter of this system as

$$\mu = \frac{M_2}{M_1 + M_2}, \tag{3}$$

and call it the *mass parameter*, assuming that $M_1 > M_2$.

In table 1, we sum up the values of all the constants for the Earth-Moon CR3PB.

System	μ	l_*	v_*	t_*
Earth-Moon	1.215×10^{-2}	$3.850 \times 10^5 \text{ km}$	1.025 km s^{-1}	$2.361 \times 10^6 \text{ s}$

TABLE 1. Table of the parameter values for the Earth-Moon system.

Equations of Motion. If we write the motion equations in a rotating frame \mathcal{R} in which the two primaries are fixed (the angular velocity is the angular velocity of their rotation around their center of mass, see [7]), we obtain that the coordinates of P_1 and P_2 are respectively

$$\chi_{P_1} = (-\mu, 0, 0, 0, 0, 0), \quad \chi_{P_2} = (1 - \mu, 0, 0, 0, 0, 0).$$

Let us call $x_1^0 = -\mu$ and $x_2^0 = 1 - \mu$, and by writing the state

$$\chi = (x, y, z, \dot{x}, \dot{y}, \dot{z})^T = (x_1, x_2, x_3, x_4, x_5, x_6)^T,$$

we obtain

$$\begin{cases} \dot{x}_1 = x_4 \\ \dot{x}_2 = x_5 \\ \dot{x}_3 = x_6 \\ \dot{x}_4 = x_1 + 2x_5 - (1 - \mu) \frac{x_1 - x_1^0}{r_1^3} - \mu \frac{x_1 - x_2^0}{r_2^3} \\ \dot{x}_5 = x_2 - 2x_4 - (1 - \mu) \frac{x_2}{r_1^3} - \mu \frac{x_2}{r_2^3} \\ \dot{x}_6 = -(1 - \mu) \frac{x_3}{r_1^3} - \mu \frac{x_3}{r_2^3} \end{cases} \quad (4)$$

where

$$r_1 = \sqrt{(x_1 - x_1^0)^2 + x_2^2 + x_3^2} \quad \text{et} \quad r_2 = \sqrt{(x_1 - x_2^0)^2 + x_2^2 + x_3^2}$$

are respectively the distances between P and primaries P_1 and P_2 .

We can define the potential

$$U(x_1, x_2, x_3) = -\frac{1}{2}(x_1^2 + x_2^2) - \frac{1 - \mu}{r_1} - \frac{\mu}{r_2} - \frac{1}{2}\mu(1 - \mu), \quad (5)$$

and we write the system as

$$\begin{cases} \dot{x}_1 = x_4 = f_1(\chi) \\ \dot{x}_2 = x_5 = f_2(\chi) \\ \dot{x}_3 = x_6 = f_3(\chi) \\ \dot{x}_4 = 2x_5 - \frac{\partial U}{\partial x_1} = f_4(\chi) \\ \dot{x}_5 = -2x_4 - \frac{\partial U}{\partial x_2} = f_5(\chi) \\ \dot{x}_6 = -\frac{\partial U}{\partial x_3} = f_6(\chi) \end{cases} \quad (6)$$

where $F_0 = (f_1, f_2, f_3, f_4, f_5, f_6)$ is the vector field of the system. We define the energy of a state point as :

$$\mathcal{E}(\chi) = \frac{1}{2}(\dot{x}^2 + \dot{y}^2 + \dot{z}^2) + U(x, y, z). \quad (7)$$

In this paper, we will consider a planar motion, hence, we only have a \mathbb{R}^4 -state in the orbital plan of the primaries.

2.2. Design of the Transfer

We want to design a mission going from a periodic Lyapunov orbit around L_1 to a periodic Lyapunov orbit around L_2 using a low-thrust engine in the Earth-Moon system (see figure 1). A full description of these periodic orbits is given in section 3.1. In order to perform such a mission, we will use the properties introduced in section 3.3: the invariant manifolds. Indeed, if we are able to find an intersection between an “ L_1 unstable manifold” and an “ L_2 stable manifold”, we get an asymptotic trajectory that perform the mission with a zero thrust, called heteroclinic orbit (see section 4.1).

In the classical literature, such a mission is usually designed by using impulse to reach the heteroclinic orbit from the Lyapunov orbit around L_1 and then another impulse to reach the Lyapunov orbit from the heteroclinic one. Since we design a low-thrust transfer, following this method is unrealistic. In [8], the author developed a three-step method to perform a low thrust low energy trajectory between Lyapunov orbits of the same energy without using invariant manifolds. At his first step, he uses a feasible quadratic-zero-quadratic control structure

to initialize his method. In this work we will use the knowledge of a zero cost trajectory, the heteroclinic orbit, to initialize an indirect shooting method (Newton-like method for optimal control problem) provided by applying the Pontryagin Maximum Principle.

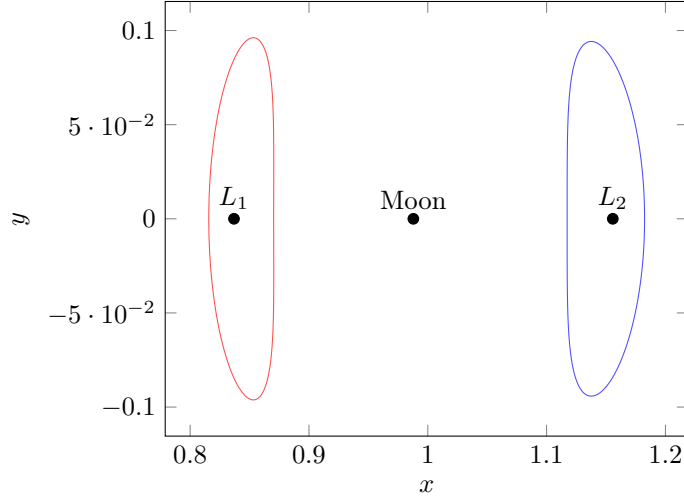


FIGURE 1. The two Lyapunov orbits around L_1 and L_2 of the Earth-Moon system, for an energy equal to -1.59208 in normalized coordinates.

2.3. Controlled Dynamics

We first describe the model for the evolution of our spacecraft in the CRTBP. In non normalized coordinates (see (8)), the controlled dynamics is the following

$$m \frac{dR}{dt} = -GM_1 m \frac{R_{13}}{R_{13}^3} - GM_2 m \frac{R_{23}}{R_{23}^3} + T(t), \quad (8)$$

where T is the spacecraft driving force, and m is the time dependant mass of the spacecraft. The equation for the evolution of the mass is

$$\dot{m}(t) = -\beta |T(t)|, \quad (9)$$

where β is computed with the two parameters I_{sp} and g_0 . Specific impulse (I_{sp}) is a measure of the efficiency of rocket and jet engines. g_0 is the acceleration at the Earth's surface. The inverse of the average exhaust speed, β , is equal to $\frac{1}{I_{sp}g_0}$.

Moreover, the thrust is constrained as follows

$$\forall t, |T(t)| \leq T_{\max}. \quad (10)$$

Using the normalization parameters (2), and denoting by β_* the normalized parameter β initially in m^{-1}s , we get the normalized controlled dynamics:

$$\left\{ \begin{array}{l} \dot{x}_1 = x_4 \\ \dot{x}_2 = x_5 \\ \dot{x}_3 = x_6 \\ \dot{x}_4 = x_1 + 2x_5 - (1 - \mu) \frac{x_1 - x_1^0}{r_1^3} - \mu \frac{x_1 - x_2^0}{r_2^3} + \frac{t_*^2}{4\pi^2 l_*} T_{\max} \frac{u_1(t)}{m(t)} \\ \dot{x}_5 = x_2 - 2x_4 - (1 - \mu) \frac{x_2}{r_1^3} - \mu \frac{x_2}{r_2^3} + \frac{t_*^2}{4\pi^2 l_*} T_{\max} \frac{u_2(t)}{m(t)} \\ \dot{x}_6 = -(1 - \mu) \frac{x_3}{r_1^3} - \mu \frac{x_3}{r_2^3} + \frac{t_*^2}{4\pi^2 l_*} T_{\max} \frac{u_3(t)}{m(t)} \\ \dot{m}(t) = -\beta_* \frac{t_*^2}{4\pi^2 l_*} T_{\max} |u(t)| \end{array} \right. \quad (11)$$

where for all t , $|u(t)| \leq 1$. In the remainder of this article, we will denote the coefficient $\frac{t_*^2}{4\pi^2 l_*} T_{\max}$ by ϵ . Hence, we get :

$$\left\{ \begin{array}{l} \dot{x}_1 = x_4 \\ \dot{x}_2 = x_5 \\ \dot{x}_3 = x_6 \\ \dot{x}_4 = x_1 + 2x_5 - (1 - \mu) \frac{x_1 - x_1^0}{r_1^3} - \mu \frac{x_1 - x_2^0}{r_2^3} + \epsilon \frac{u_1(t)}{m(t)} \\ \dot{x}_5 = x_2 - 2x_4 - (1 - \mu) \frac{x_2}{r_1^3} - \mu \frac{x_2}{r_2^3} + \epsilon \frac{u_2(t)}{m(t)} \\ \dot{x}_6 = -(1 - \mu) \frac{x_3}{r_1^3} - \mu \frac{x_3}{r_2^3} + \epsilon \frac{u_3(t)}{m(t)} \\ \dot{m}(t) = -\beta_* \epsilon |u(t)| \end{array} \right. \quad (12)$$

In short, we write the system as :

$$\left\{ \begin{array}{l} \dot{x} = F_0(x) + \frac{\epsilon}{m} \sum_{i=1}^2 u_i F_i(x), \\ \dot{m} = -\beta_* \epsilon |u|, \end{array} \right. \quad (13)$$

where F_0 is defined in (6) restricted to the four dimensional dynamics, and

$$F_1(x) = \begin{pmatrix} 0 \\ 0 \\ 1 \\ 0 \end{pmatrix}, \quad F_2(x) = \begin{pmatrix} 0 \\ 0 \\ 0 \\ 1 \end{pmatrix}.$$

Controllability. [5] proved that the CRTBP with a non evolving mass is controllable:

Theorem 2.1. *For any $\mu \in (0, 1)$, for any positive ϵ , the circular restricted three-body problem is controllable on the phase space.*

Using proposition (2.2) in [4], one can extend this results to the system with an evolving mass.

2.4. Optimal Control Problem (OCP)

Our main goal in this work is to solve an optimal control problem. We want to go from the Lyapunov orbit around L_1 to the Lyapunov orbit around L_2 with minimal energy. Mathematically we write this problem as follows

$$\mathcal{P}_g \begin{cases} \mathcal{C}_g = \min \int_0^{t_f} \|u\|^2 dt, \\ \dot{x} = F_0(x) + \frac{\epsilon}{m} \sum_{i=1}^2 u_i F_i(x), \\ \dot{m} = -\beta_* \epsilon |u|, \\ |u| \leq 1, \\ x(0) \in \text{Lya}_1, \text{ and } x(t_f) \in \text{Lya}_2. \end{cases} \quad (14)$$

We are going to present the method we developed to solve this problem. Let us summarize the steps we follow:

- First, we find a heteroclinic orbit from the Lyapunov orbit around L_1 to the Lyapunov orbit around L_2 .
- Then, we realize a short transfer from a *fixed point* on the Lyapunov orbit around L_1 to the heteroclinic orbit.
- Similarly, we realize a transfer from the heteroclinic orbit to a *fixed point* on the Lyapunov orbit around L_2 .
- Then we release the constraint on the position of the matching connections on the heteroclinic orbit using a multiple shooting method and we decrease the maximal thrust.
- Finally, we optimize the position of the two fixed points on Lya_1 and Lya_2 to satisfy the transversality condition for problem (14).

We can note that in the three first steps where we are solving optimal control problems, we have fixed the departure and arrival points to simplify the problem. The last step consists in releasing these constraints.

3. PROPERTIES OF CRTBP

In this Section, we recall some properties of the CRTBP. In particular, we introduce equilibrium points, Lyapunov orbits and invariant manifolds. We explain how to numerically compute these orbits (see Section 3.2). We have improved the method used in [2] using the energy as continuation parameter. Finally, we introduce the invariant manifolds and how we can get a numerical approximation.

3.1. Lyapunov Orbits

Equilibrium Points. The Lagrange points are the equilibrium points of the circular restricted three-body problem. Euler [9] and Lagrange [19] proved the existence of five equilibrium points: three collinear points on the axis joining the center of the two primaries, generally denoted by L_1 , L_2 and L_3 , and two equilateral points denoted by L_4 and L_5 (see figure 2).

Computing equilateral points L_4 and L_5 is not very complicated, but it is not possible to find exact solutions for collinear equilibria L_1 , L_2 and L_3 . A lot of efforts has been dedicated to find the series expansion for these points. We used solutions from [25], and we write here only the two solutions that we will use:

$$\begin{aligned} \gamma_1 &= r_h \left(1 - \frac{1}{3} r_h - \frac{1}{9} r_h^2 + \dots \right), \\ \gamma_2 &= r_h \left(1 + \frac{1}{3} r_h - \frac{1}{9} r_h^2 + \dots \right), \end{aligned} \quad (15)$$

for $L_1 = (\gamma_1, 0, 0)$ and $L_2 = (\gamma_2, 0, 0)$. We recall that the collinear points are shown to be unstable (in every system), whereas L_4 and L_5 are proved to be stable under some conditions (see [20]).

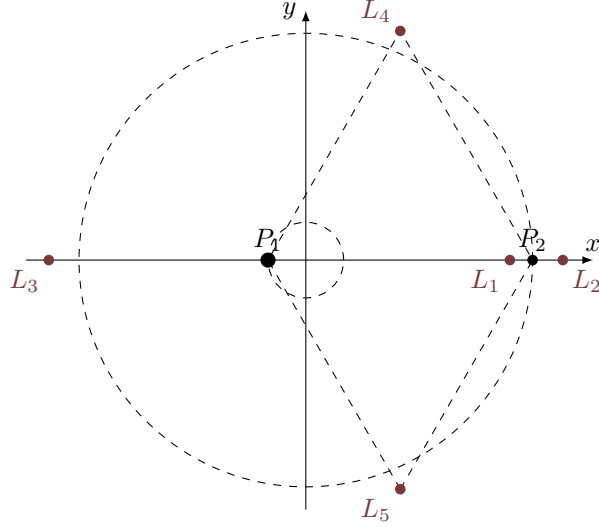


FIGURE 2. Localisation of Lagrange's points.

Lyapunov Orbits. Let us focus on the three collinear equilibrium points. It is standard to expand the nonlinear terms $\frac{1}{r_1}$ and $\frac{1}{r_2}$ as series in Legendre polynomials, using the formula :

$$\frac{1}{\sqrt{(x-A)^2 + (y-B)^2 + (z-C)^2}} = \frac{1}{D} \sum_{n=0}^{\infty} \left(\frac{\rho}{D}\right)^n P_n \left(\frac{Ax + By + Cz}{D\rho}\right), \quad (16)$$

where $D^2 = A^2 + B^2 + C^2$, $\rho^2 = x^2 + y^2 + z^2$ and P_n is the Legendre polynomial of degree n . Then, using a coordinate system centered in the equilibrium point¹ L_i , $i = 1, 2, 3$, the equations of motion (4) can be written as

$$\begin{cases} \ddot{x} - 2\dot{y} - (1 + 2c_2)x = \frac{\partial}{\partial x} \sum_{n \geq 3} c_n \rho^n P_n \left(\frac{x}{\rho}\right), \\ \ddot{y} + 2\dot{x} - (c_2 - 1)y = \frac{\partial}{\partial y} \sum_{n \geq 3} c_n \rho^n P_n \left(\frac{x}{\rho}\right), \\ \ddot{z} + c_2 z = \frac{\partial}{\partial z} \sum_{n \geq 3} c_n \rho^n P_n \left(\frac{x}{\rho}\right), \end{cases} \quad (17)$$

where

$$c_n = \frac{1}{\gamma_i^{n+1}} \left(\mu + \frac{(1 - \mu)\gamma_i^{n+1}}{(1 - \gamma_i)^{n+1}} \right).$$

As previously, γ_i denotes the distance between the Lagrange point L_i and the second primary.

Hence, at Lagrange points L_i , $i = 1, 2, 3$, the linearized system of (17) is

$$\begin{cases} \ddot{x} - 2\dot{y} - (1 + 2c_2)x = 0, \\ \ddot{y} + 2\dot{x} - (c_2 - 1)y = 0, \\ \ddot{z} + c_2 z = 0. \end{cases} \quad (18)$$

¹This system is called the Richardson system.

This is of the kind saddle \times center \times center. Indeed, a simple computation leads to the eigenvalues $(\pm\lambda, \pm i\omega_p, \pm i\omega_v)$:

$$\lambda^2 = \frac{c_2 - 2 + \sqrt{9c_2^2 - 8c_2}}{2}, \quad \omega_p^2 = \frac{c_2 - 2 - \sqrt{9c_2^2 - 8c_2}}{2}, \quad \text{et} \quad \omega_v^2 = c_2.$$

The following theorem ensures the existence of periodic orbits around equilibrium points (see [3, 20] and references therein).

Theorem 3.1 (Lyapunov-Poincaré). *Let $\dot{x} = H(x)$ be a hamiltonian system in \mathbb{R}^{2n} , x_0 an equilibrium point identified to 0, and $A = \frac{\partial H}{\partial x}(0)$ the linearized system matrix. Assume that the eigenvalues of A are*

$$\sigma(A) = \{\pm i\omega, \lambda_3, \dots, \lambda_{2n}\},$$

where $\omega > 0$.

If $\lambda_j/i\omega \notin \mathbb{Z}$ for $j \in \llbracket 3, 2n \rrbracket$, then there exists a one-parameter family of periodic orbits around 0. Moreover, when approaching the equilibrium point along the family, the periods tend to $2\pi/\omega$ and the nontrivial multipliers tend to $\exp(2\pi\lambda_j/\omega)$, $j \in \llbracket 3, 2n \rrbracket$.

In this work, we only consider a planar motion. In this case applying this theorem to the collinear points L_1 , L_2 and L_3 we get a one-parameter family of periodic orbits around each of these equilibrium points. These periodic orbits are called Lyapunov orbits and are homeomorphic to a circle. In this work, we denote by Lya_i a Lyapunov orbit around the equilibrium point L_i . For the spatial case, orbits are called Halo orbits or Lissajous orbits (for instance, see [14]).

Numerical computation. We will describe the method to compute Lyapunov orbits around collinear Lagrange points. To find these periodic orbits, we use Newton-like method. Since equations in the coordinate system centered on L_i are symmetric, if we consider a periodic solution of (17), $\chi(t) = (x(t), y(t), \dot{x}(t), \dot{y}(t))$ of period t_χ , then there exists t_0 such that

$$\begin{cases} x(t_0) = x_0, \\ y(t_0) = 0, \\ \dot{x}(t_0) = 0, \\ \dot{y}(t_0) = \dot{y}_0, \end{cases} \quad \text{and} \quad \begin{cases} x(t_0 + t_\chi/2) = x_1, \\ y(t_0 + t_\chi/2) = 0, \\ \dot{x}(t_0 + t_\chi/2) = 0, \\ \dot{y}(t_0 + t_\chi/2) = \dot{y}_1. \end{cases}$$

Since t_0 could be chosen to be equal to zero and fixing x_0 , we just have to find (\dot{y}_0, t_χ) such that, denoting by ϕ the flow of the dynamical system, and $\chi_0 = (x_0, 0, 0, \dot{y}_0)$, the function \mathcal{S}_L satisfies:

$$\mathcal{S}_L(t_\chi, \dot{y}_0) = \begin{pmatrix} \phi_2(t_\chi/2, \chi_0) \\ \phi_3(t_\chi/2, \chi_0) \end{pmatrix} = \begin{pmatrix} 0 \\ 0 \end{pmatrix}. \quad (19)$$

In practice, we fix for example the value of x_0 in order to be left with finding a zero of a function in \mathbb{R}^2 of two variables (\dot{y}_0, t_χ) . Obviously, we can extend this to a periodic orbit in \mathbb{R}^6 .

The main difficulty is to initialize the Newton-like algorithm. The idea is to find an analytical approximation of the orbit to a certain order, and then inject this into the Newton-like algorithm. In this work, and because the Lyapunov orbit is not very difficult to compute, we follow [24]. For various orbits in \mathbb{R}^6 , see [2, 10, 16] and references therein.

3.2. Computing the family

In order to use these orbits to construct the targeted mission, it is very useful to be able to compute the family of periodic orbits, providing us with different orbits that have different energies.

3.2.1. Continuation methods

To explain how we get the family of periodic orbits, let us introduce continuation methods, for a more complete introduction, see [1]. The main idea is to construct a family of problems denoted by $(\mathcal{P}_\lambda)_{\lambda \in [0,1]}$ depending on a parameter $\lambda \in [0,1]$. The initial problem \mathcal{P}_0 is supposed to be easy to solve, and the final problem \mathcal{P}_1 is the one we want to solve.²

Let us suppose that we have solved numerically \mathcal{P}_0 , and consider a subdivision $0 = \lambda_0 < \lambda_1 < \dots < \lambda_p = 1$ of the interval $[0,1]$. The solution of \mathcal{P}_0 can be used to initialize the Newton-like method applied to \mathcal{P}_{λ_1} . And so on, step by step, we use the solution of $\mathcal{P}_{\lambda_{i-1}}$ to initialize \mathcal{P}_{λ_i} . Of course, the sequence (λ_i) has to be well chosen and eventually should be refined.

Mathematically, for this method to converge, we need that the family of problems to depend continuously on the parameter λ . See [3, chap. 9] for some justification of the method.

From the numerical point of view, there exist many methods and strategies in order to implement continuation or homotopy methods. We can distinguish between differential pathfollowing, simplicial methods, predictor-corrector methods, etc. In this work, we implement a predictor-corrector method because it is suitable for our problem. We can note that there exist many codes which can be found on the web, such as the well-known Hompack90 [29] or Hampath [6]. For a survey about different results, challenges and issues on continuation methods, see [27].

3.2.2. Application to the family of orbits

Since we had to choose a parameter x_0 to write the zero function \mathcal{S}_L in (19), it is natural to use this parameter to perform our continuation that computes the family of orbits. Indeed, we can choose to reach a certain x_0^{obj} . So we can define our continuation as :

$$\mathcal{P}_\lambda : \begin{cases} \text{for } x_0^\lambda = (1-\lambda)x_0 + \lambda x_0^{\text{obj}} \\ \mathcal{S}_L^\lambda(t_\chi, \dot{y}_0) = \begin{pmatrix} \phi_2(t_\chi/2, \chi_0^\lambda) \\ \phi_3(t_\chi/2, \chi_0^\lambda) \end{pmatrix} = \begin{pmatrix} 0 \\ 0 \end{pmatrix} \end{cases}$$

where $\chi_0^\lambda = (x_0^\lambda, 0, 0, \dot{y}_0)$. Thanks to the analytical approximation provided by [24] or [16], we can solve the initial problem \mathcal{P}_0 . Using the continuation method described previously, we can get a family of periodic orbit.

However, for some periodic orbits (halo family), we can observe that the continuation fails when we converge to the equilibrium point ($x_0^{\text{obj}} \rightarrow 0$). A much better continuation parameter is *energy*. It releases the constraint on the parameter x_0 , and allows us to reach any periodic orbit, in particular the algorithm converges to the energy of L_i , $i \in \{1, \dots, 3\}$. Moreover, it is a significantly more natural parameter, keeping in mind that we will construct a controlled transfer method. Section 3.3 will provide an extra argument in favor of the energy parameter.

Thanks to the analytical approximation, we get a first periodic orbit with energy \mathcal{E}_0 , then we want to reach a prescribed energy \mathcal{E}_1 . So we define the following family of problems:

$$\mathcal{P}_\lambda^\mathcal{E} : \mathcal{S}_\mathcal{E}^\lambda(t_\chi, x_0, \dot{y}_0) = \begin{pmatrix} \phi_2(t_\chi/2, \chi_0) \\ \phi_3(t_\chi/2, \chi_0) \\ \mathcal{E}(\chi_0) = \mathcal{E}_\lambda \end{pmatrix} = \begin{pmatrix} 0 \\ 0 \\ 0 \end{pmatrix} \quad (20)$$

where $\mathcal{E}(\chi_0)$ is the energy of the trajectory starting at χ_0 and

$$\mathcal{E}_\lambda = (1-\lambda)\mathcal{E}_0 + \lambda\mathcal{E}_1.$$

For more details, see algorithm 1. Here we just use a predictor-corrector continuation (see [1]).

Figure 3 shows an example of a family of Lyapunov orbits around L_1 in the Earth-Moon system.

²Usually when the dependency on the parameter λ is linear, we speak about *continuation method* and when it is not the case we speak about *homotopy methods*.

Algorithm 1 Orbit Continuation Algorithm

Require: \mathcal{E}_1 : objective energy, $\epsilon_{\min} > 0$, ϵ_{\min} and ϵ_{\max} .

Require: $\chi_0 = (x_0, 0, 0, \dot{y}_0)$ and t_χ provided by analytical approximation.

- 1: $\mathcal{E}_0 = \mathcal{E}(\chi_0)$, $\lambda = 0$.
 - 2: $x_s = x_0$, $\dot{y}_s = \dot{y}_0$ and $t_s = t_\chi$.
 - 3: $i = 0$.
 - 4: **while** $\lambda < 1$ and $\epsilon > \epsilon_{\min}$ **do**
 - 5: $\epsilon = \min(\epsilon, 1 - \lambda)$
 - 6: we increase : $\lambda = \lambda + \epsilon$.
 - 7: we initialize : $(t_c, x_c, \dot{y}_c) \leftarrow (t_s, x_s, \dot{y}_s)$
 - 8: $\mathcal{E}_\lambda = (1 - \lambda)\mathcal{E}_0 + \lambda\mathcal{E}_1$
 - 9: Newton-like Method to solve $\mathcal{S}_\mathcal{E}^\lambda(t_c, x_c, \dot{y}_c) = 0$.
 - 10: **if** success **then**
 - 11: we keep the solution : $(t_s, x_s, \dot{y}_s) \leftarrow (t_c, x_c, \dot{y}_c)$
 - 12: we increase : $\epsilon = \min(\alpha\epsilon, \epsilon_{\max})$, $\alpha > 1$.
 - 13: **else**
 - 14: we decrease : $\epsilon = \beta\epsilon$, $\beta < 1$.
 - 15: **end if**
 - 16: **end while**
-

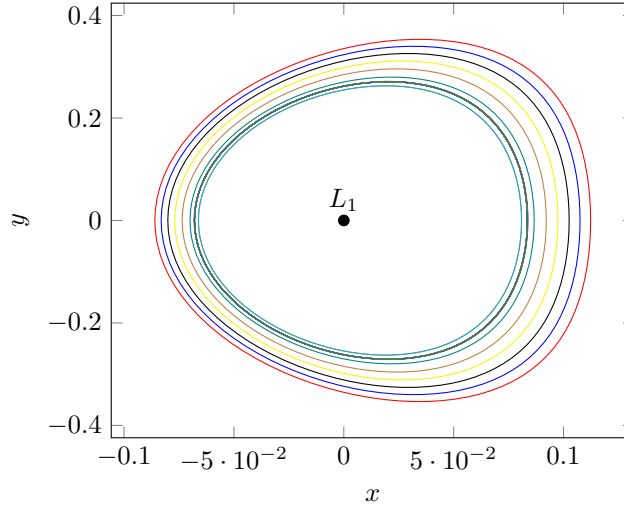


FIGURE 3. A family of Lyapunov orbits around L_1 in the Earth-Moon system (Richardson coordinates)

3.3. Invariant Manifolds

All the periodic orbits described in the previous section come with their invariant manifolds, that is to say, the sets of phase points from which the trajectory converges to the periodic orbit, forward for the *stable* manifold and backward for the *unstable* manifold. These manifolds can be very useful to design interplanetary mission because as separatrix, they are some sort of gravitational current. We refer to [17, chap. 4] for the proof of existence and a more detailed explanation of these manifolds.

Monodromy Matrix. We introduce a tool of dynamical systems: the monodromy matrix. Some properties of this matrix are needed to numerically compute the invariant manifolds. For more details, see [17, 20].

Let $\bar{x}(\cdot)$ be a periodic solution of the dynamical system with period T and $\bar{x}(0) = \bar{x}_0$. Denoting by ϕ the flow of the system, the monodromy matrix M of the periodic orbit for the point \bar{x}_0 is defined as

$$M = \frac{\partial \phi(T; \bar{x}_0)}{\partial x_0}. \quad (21)$$

It determines whether initial perturbations $\delta \bar{x}_0$ of the periodic orbit decay or grow. Indeed, if we define

$$\delta \bar{x}(T) = \phi(T; \bar{x}_0 + \delta \bar{x}_0) - \phi(T; \bar{x}_0),$$

we have, at the first order

$$\delta \bar{x}(T) = \frac{\partial \phi(T; \bar{x}_0)}{\partial x_0} \delta \bar{x}_0.$$

Local Approximation to Compute Invariant Manifolds. Using the Poincaré map we can show that the eigenvectors corresponding to eigenvalues of the monodromy matrix are linear approximations of the invariant manifolds of the periodic orbit. For the planar Lyapunov orbits in the CRTBP, we show that the four eigenvalues of M are :

$$\lambda_1 > 1, \quad \lambda_2 = \frac{1}{\lambda_1}, \quad \lambda_3 = \lambda_4 = 1.$$

The eigenvector associated with the eigenvalue λ_1 is in the unstable direction and the eigenvector associated with the eigenvalue λ_2 is in the stable direction.

Then, the method to compute invariant manifolds is the following:

- (1) First, for χ_0 a point of the periodic orbit, we compute the monodromy matrix and its eigenvectors. Let's denote by $Y^s(\chi_0)$ the normalized stable eigenvector and by $Y^u(\chi_0)$ the normalized unstable eigenvector.
- (2) Then, let

$$\begin{aligned} \chi^{s\pm}(\chi_0) &= \chi_0 \pm \alpha Y^s(\chi_0), \\ \chi^{u\pm}(\chi_0) &= \chi_0 \pm \alpha Y^u(\chi_0), \end{aligned} \quad (22)$$

be the initial guesses for (respectively) the stable and unstable manifolds. The magnitude of α should be small enough to be within the validity of the linear estimate but not too small to keep a reasonable time of escape or convergence (for instance, see [15] for a discussion on the value of α).

- (3) Finally, we integrate numerically the unstable vector forward in time, using both α and $-\alpha$ to generate the two branches of the unstable manifold denoted by $W^{u\pm}(\chi_0)$. We do the same for the stable vector backwards, and we get the two branches of stable manifold $W^{s\pm}(\chi_0)$ (see figure 4).

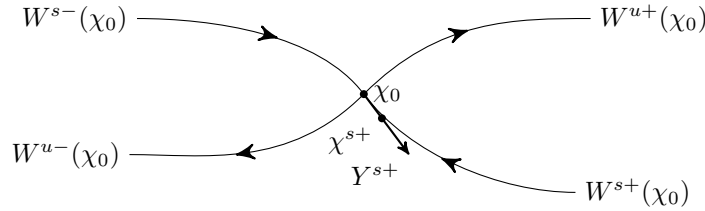


FIGURE 4. Illustration of the method to compute invariant manifolds.

Following this process, we are able to compute the invariant manifolds of any Lyapunov orbit of any energy (greater than the energy of L_i , for an explanation of that, see the section about Hill regions in [17]). We have represented parts of these manifold for a Lyapunov orbit in the Earth-Moon system at energy -1.59208 in normalized coordinates in figure 5.

These manifolds are very useful to design interplanetary transfer with low consumption. Indeed, they are separatrices of the dynamics, these manifolds can be seen as gravitationnal currents. In section 2, we will explain how we can use the manifolds in practice.

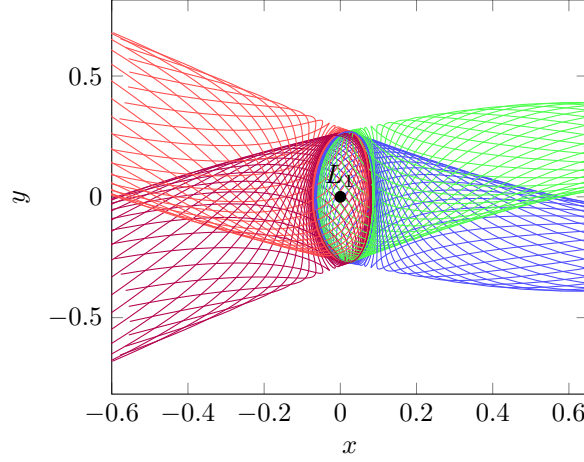


FIGURE 5. Manifolds of a Lyapunov orbit around L_1 of the Earth-Moon system and Richardson coordinates. The energy of these orbit and manifolds is -1.59208 in normalized coordinates (centered on the barycenter of the two primaries).

Remark: Since we are following invariant manifolds converging in infinite time to the periodic orbits (backwards or forward), and because we are doing it numerically and so with a certain approximation, there exist long times for which we cannot manage to converge. We have to tune the parameter α in (22) (we give in section 4.1 the choice of the numerical value). Moreover, the multiple shooting method allows to subdivide the time and keep each part to reasonable time of integration.

4. CONSTRUCT THE MISSION

In this section we explain all the steps of our method solving the problem 14. We first find a heteroclinic orbit between the two Lyapunov orbits. Then we perform two short transfers from L_{y1} to the heteroclinic orbit, and from the heteroclinic orbit to L_{y2} . Then, with a multiple shooting method we release the constraint on the position of the matching connections on the heteroclinic. Finally, we optimize the departure and arrival points previously fixed to simplify the problem.

4.1. The Heteroclinic Orbits

Let us first find the heteroclinic orbit between a Lyapunov orbit around L_1 and a Lyapunov orbit around L_2 . One condition to be able to find such an orbit is to compute an intersection between two manifolds. Hence, these two manifolds should have the same energy. Since the manifold and the Lyapunov orbit have the same energy, we must compute two Lyapunov orbits around L_1 and L_2 with a given energy.

The study of the well known Hill regions (see [17] and references therein), *i.e.* the projection of the energy surface of the uncontrolled dynamics onto the position space gives us an indication of the interval of energy we can use. Indeed, we have to compute an orbit with an energy greater than the L_2 energy. And because we want to realize a low-thrust transfer, we choose to keep a low energy. Moreover, we have a smaller region of possible motion, and so, a possibly shorter transfer.

Using the method described in 3.2.2, we choose to get two orbits with an energy of -1.592081 in the normalized system. The main difficulty is to find a value of the energy for which the intersection exists. Finding the intersection. To find an intersection, we define two 2D sections U_2 , defined as

$$U_2 = \{(x, y) \in \mathbb{R}^2, x = 1 - \mu, y < 0\},$$

and U_3 defined as

$$U_3 = \{(x, y) \in \mathbb{R}^2, x = 1 - \mu, y > 0\}.$$

We represent them in figure 6.

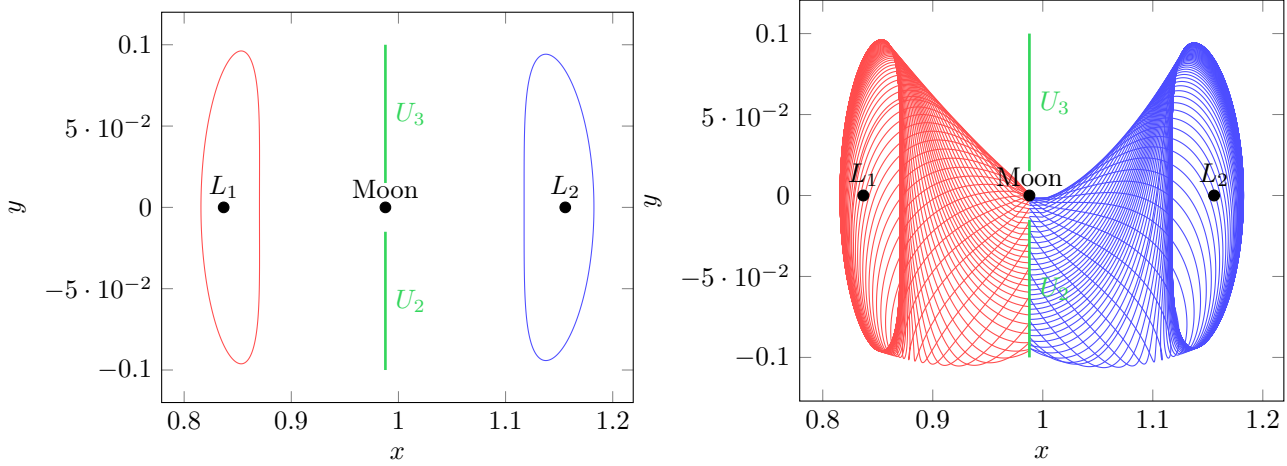


FIGURE 6. On the left: Planes U_2 and U_3 in the Earth-Moon system. On the right, unstable (red) and stable (blue) manifolds respectively from L_1 and L_2 stopping at the plane U_2

Then, we compute the intersection of the stable manifold from L_1 and the unstable manifold from L_2 with the space U_2 (of course, we can do the symmetric counterpart: unstable manifold from L_1 and stable manifold from L_2 with the space U_3). Since the x -coordinate is fixed by U_2 and because the energies of the two manifolds are equal, we just have to compute the intersection in the (y, \dot{y}) -plan (values of \dot{x} are deduced from the energy equation (7)).

We show in figure 7 the U_2 -section and the existence of intersections for our particular energy. To find precisely one intersection point, we have used once more a Newton-like method. We can parametrize the section of one manifold with U_2 with only one parameter, the parameter of the Lyapunov orbit. We denote by $\phi_{x=1-\mu}^+$, the flow propagating forward a state point from Lya_1 onto the space U_2 , and by $\phi_{x=1-\mu}^-$ the flow propagating backward a state point from Lya_2 onto the plan U_2 . Time of propagation is fixed by the condition $x = 1 - \mu$.

We want to find two points $\chi_{L_1} \in \text{Lya}_1$ and $\chi_{L_2} \in \text{Lya}_2$ such that

$$\phi_{x=1-\mu}^+(\chi^{u+}(\chi_{L_1})) - \phi_{x=1-\mu}^-(\chi^{s-}(\chi_{L_2})) = 0,$$

where χ^{u+} and χ^{s-} are defined in 22. This is an equality in \mathbb{R}^2 , and because each of the Lyapunov orbits is parametrized with a one dimensional parameter (the time), our problem is well posed.

To initialize the method we use a discretisation (100 points in this particular example) of the Lyapunov orbits and we take the two points minimizing the Euclidean norm in the U_2 section.

In our case, with a value of energy equal to -1.592081 and $\alpha = \frac{1}{384402}$, we obtain the heteroclinic trajectory represented in figure 8. From now on, we will denote this heteroclinic orbit by Het. Note that this computation only take few seconds on a standard desktop computer.

4.2. From One Orbit to Another

Here, we construct two simpler problems: first we compute an optimal control using the Pontryagin Maximum Principle reaching the heteroclinic orbit from the Lyapunov orbit around L_1 , then we compute an optimal control to reach the Lyapunov orbit around L_2 from the heteroclinic orbit. In this way, we get an admissible control that follows the null control heteroclinic orbit during a certain time.

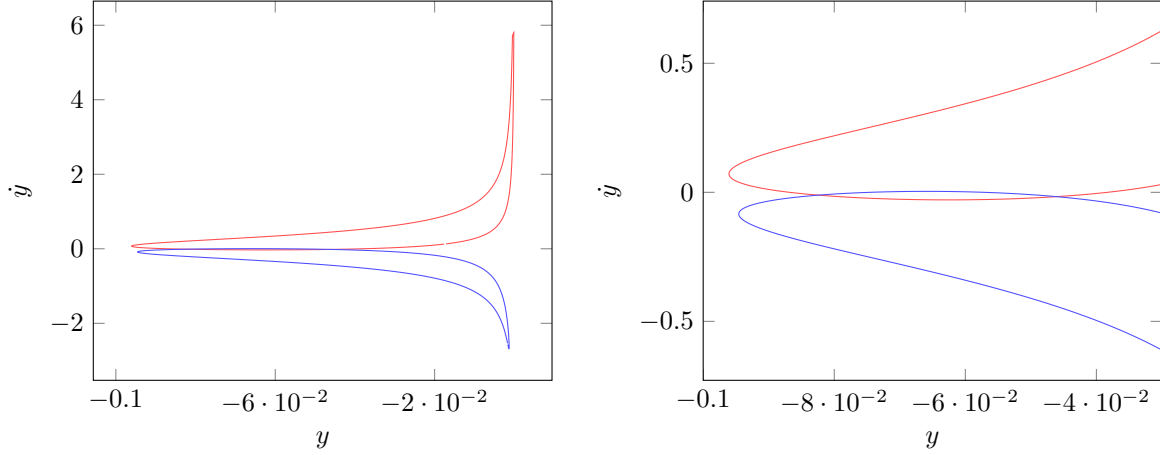


FIGURE 7. Section in the section U_2 of a unstable manifold from L_1 and a stable manifold from L_2 . The energy is -1.592081 . On the right, a zoom on the interesting area.

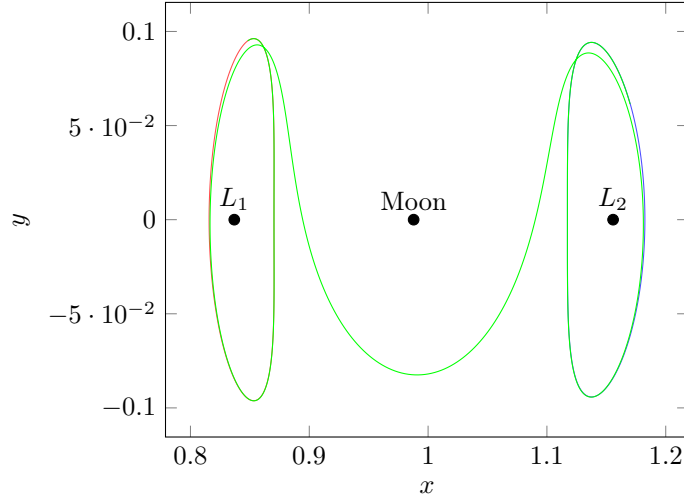


FIGURE 8. Heteroclinic orbit between two Lyapunov orbits in the Earth-Moon system. We get a travel time of 8.9613933501964 (normalized time) or 38.974 days.

4.2.1. Around L_1

Problem Statement. Consider two points $\chi_0^* \in \text{Lya}_1$ and $\chi_1^* \in \text{Het}$, a time t_0 and an initial mass $m_0^* = 1500$ kg. We apply the Pontryagin Maximum Principle to the following problem:

$$\mathcal{P}_{L_1} \begin{cases} \min \int_0^{t_0} \|u\|^2 dt, \\ \dot{x} = F_0(x) + \frac{\epsilon}{m} \sum_{i=1}^2 u_i F_i(x), \\ \dot{m} = -\beta_* \epsilon |u|, \\ |u| \leq 1, \\ x(0) = \chi_0^*, m(0) = m_0^* \text{ and } x(t_0) = \chi_1^*. \end{cases} \quad (23)$$

Here, we have fixed the two points χ_0^* and χ_1^* on the Lyapunov orbit and the heticlinic orbit. We will see how we choose these points later. We will release the constraint on the position of these two points by an optimization and satisfy the transversality conditions for problem 14 in the last steps of our method.

Since the two points χ_0^* and χ_1^* belong to trajectories with an energy greater than $\mathcal{E}(L_2) > \mathcal{E}(L_1)$, we know that an admissible trajectory connecting χ_0^* to χ_1^* exists (see [7]).

If t_0 is greater than the *minimum time*, we can show that we are in the *normal* case for the Pontryagin Maximum Principle, that is to say p^0 can be normalized to -1 (see proposition 2 in [5]). Although we have not proved that this assumption holds, we will see that it is a reasonable one because of the construction of our two points.

We define the Hamiltonian as:

$$\mathcal{H}(x, m, p, p_m, u) = -\|u\|^2 + \langle p, F(x) \rangle - \langle p_m, \beta_* \epsilon |u| \rangle,$$

where $F(x) = F_0(x) + \frac{\epsilon}{m} \sum_{i=1}^2 u_i F_i(x)$, $p \in \mathbb{R}^4$ and $p_m \in \mathbb{R}$.

To simplify the notation, we write:

$$\mathcal{H}(x, m, p, p_m, u) = -\|u\|^2 + H_0 + H_1 + H_2 - \langle p_m, \beta_* \epsilon |u| \rangle, \quad (24)$$

where $H_i = \langle p, F_i(x) \rangle$, $i = 0, \dots, 2$.

Let us define $\varphi(p) = (p_3, p_4)$, thanks to the maximization condition of the Pontryagin Maximum Principle, we get the optimal control. Denoting by $y = (x, m, p, p_m)$, let us introduce the *switch function*:

$$\psi(y) = \frac{-\beta_* \epsilon p_m - \epsilon/m |\varphi(p)|}{2}. \quad (25)$$

Then, the control is:

- if $|\varphi(p)| \neq 0$, then

$$\begin{cases} u(y) = 0 & \text{if } \psi(y) \leq 0, \\ u(y) = \psi(y) \frac{\varphi(p)}{|\varphi(p)|} & \text{if } \psi(y) \in [0, 1], \\ u(y) = \frac{\varphi(p)}{|\varphi(p)|} & \text{else,} \end{cases} \quad (26)$$

- if $|\varphi(p)| = 0$, then

$$\begin{cases} u(y) = 0 & \text{if } \psi(y) \leq 0, \\ u(y) \in \mathbf{S}(0, \psi(y)) & \text{if } \psi(y) \in [0, 1], \\ u(y) \in \mathbf{S}(0, 1) & \text{else,} \end{cases} \quad (27)$$

where $\mathbf{S}(a, b)$ is the \mathbb{R}^2 -sphere centered in a with radius b .

In this problem, let us write the transversality conditions from the Pontryagin Maximum Principle for the first problem (23). The free mass at the end of the transfer gives us : $p_m(t_0) = 0$. Moreover, because of the final condition $x(t_0) = \chi_1^*$, $p(t_0)$ is free. Finally, we are left to find $(p(0), p_m(0))$ such that the final state condition is satisfied.

We can write this problem as a shooting function. We denote by ϕ^{ext} the extremal flow of the extremal system. Hence, we define the shooting function:

$$\mathcal{S}_{L_1}(p(0), p_m(0)) = \begin{pmatrix} \phi_{1,\dots,4}^{\text{ext}}(\chi_0^*, m_0^*, p(0), p_m(0)) - \chi_1^* \\ \phi_{10}^{\text{ext}}(\chi_0^*, m_0^*, p(0), p_m(0)) \end{pmatrix} = \begin{pmatrix} 0 \\ 0 \end{pmatrix}. \quad (28)$$

We compute the solution, that is to say $p(0)$ and $p_m(0)$ using a shooting method (Newton-like method applied to (28)). As is well known, the main difficulty is to *initialize* the Newton-like algorithm. To do this, we have used a continuation method. Let us explain the process.

Construction of χ_0^* and χ_1^* . Let us recall that we want to realize the transfer from Lya_1 to Het. We have already computed the heteroclinic orbit. The method is the following:

- (1) If we denote by $\chi_{\text{Het}}^{L_1}$ the first point of the “numerical” heteroclinic orbit near the Lypunov orbit, we find $\chi_{\text{Lya}_1} \in \text{Lya}_1$ by minimizing the euclidian norm : $\chi_{\text{Lya}_1} = \arg \min_{\chi \in \text{Lya}_1} \left\| \chi_{\text{Het}}^{L_1} - \chi \right\|$.
- (2) Then, we propagate backward in time χ_{Lya_1} following the uncontrolled dynamics during a time t_{Lya_1} (smaller than the period of the Lyapunov orbit) to get χ_0^*
- (3) We propagate forward in time $\chi_{\text{Het}}^{L_1}$ during a reasonable time $t_{\text{Het}}^{L_1}$ to get χ_1^* (small compared to the traveling time to reach the other extremity of Het).

We define the transfer time t_0 in (23) as

$$t_0 = t_{\text{Lya}_1} + t_{\text{Het}}^{L_1}.$$

Although it seems to be a simpler problem than problem (14), the main difficulty is still to initialize the shooting method. We use a continuation method on the final state, using as a first simpler problem a natural trajectory corresponding to a null control. Then step by step, we reach the targeted final point on the heteroclinic orbit.

Final State Continuation. As explained in section 3.2.1, we construct a family of problems \mathcal{P}_λ depending continuously on one parameter λ such that \mathcal{P}_0 is easy to solve and \mathcal{P}_1 corresponds to the targeted problem, that is to say (23).

First, let us define $\chi_{\text{Lya}_1}^{\text{nat}}$ as the forward propagation of χ_{Lya_1} following the uncontrolled dynamics during time t_0 . Then we define the family of problems:

$$\mathcal{P}_{L_1}^\lambda \begin{cases} \min \int_0^{t_0} \|u\|^2 dt, \\ \dot{x} = F_0(x) + \frac{\epsilon}{m} \sum_{i=1}^2 u_i F_i(x), \\ \dot{m} = -\beta_* \epsilon |u|, \\ |u| \leq 1, \\ x(0) = \chi_0^*, \quad m(0) = m_0^*, \\ x(t_0) = (1 - \lambda)\chi_{\text{Lya}_1}^{\text{nat}} + \lambda\chi_1^*. \end{cases} \quad (29)$$

Since $\chi_{\text{Lya}_1}^{\text{nat}}$ corresponds to an uncontrolled dynamics, the corresponding initial costate $(p(0), p_m(0))$ is zero.

Then, step by step, we initialize the shooting method of $\mathcal{P}_{L_1}^{\lambda_i}$ using the solution of $\mathcal{P}_{L_1}^{\lambda_{i-1}}$ to reach problem (23).

Figure 9 shows the different points defined for some parameters described below.

Numerical Results. We show here the numerical results for this transfer. We choose a maximal thrust equal to 60 N. We postpone to section 4.3 the problem of the maximum thrust which should be very small. In fact, a high thrust implies that the magnitude of the costate stays very low, and it will be necessary for the multiple shooting to converge. Moreover, we choose the two times of propagation in the normalized system as:

$$t_{\text{Lya}_1} = 1.0, \quad t_{\text{Het}}^{L_1} = 2.0.$$

We obtain the optimal trajectory plotted in figure 9. The optimal command is shown in figure 10. One can see that we are far from the saturation of the command, indeed, the maximum value is approximately $6e-06$, whereas we are constrained by one. We postpone the discussion on the real value in Newton to the final trajectory.

This continuation gives us an initial adjoint vector (costate) that we will denote by p_0^* and p_m^{0*} in the remainder of this work.

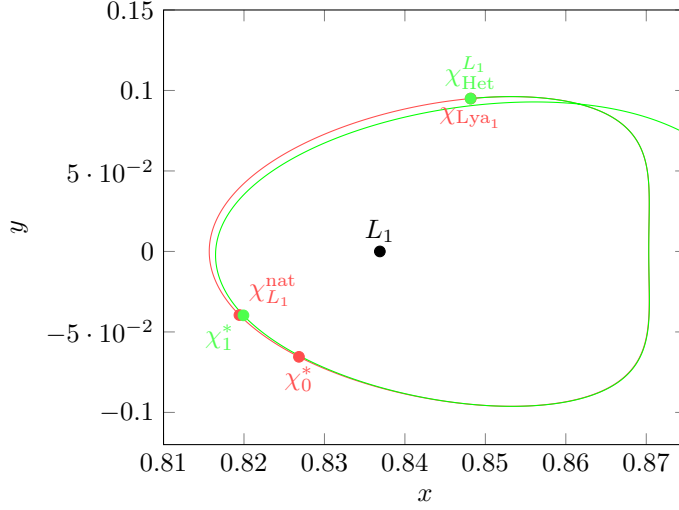
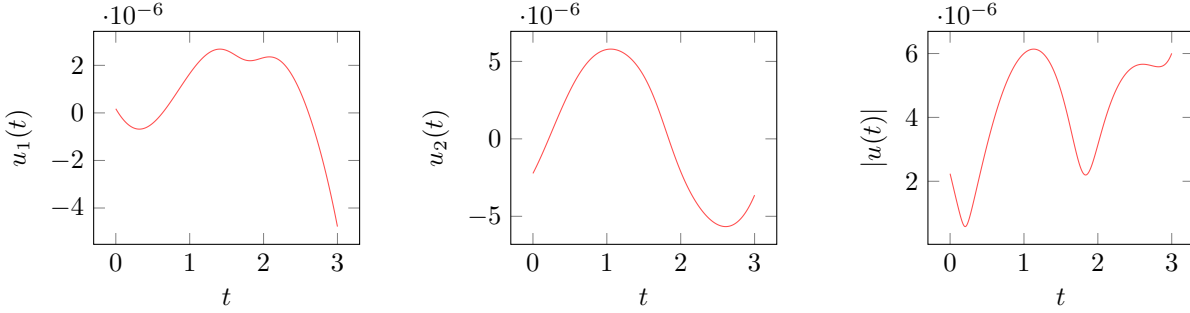


FIGURE 9. All different points in the construction of the problem.

FIGURE 10. Command to realize the optimal transfer from the Lyapunov orbit to the heteroclinic orbit. We plot $u(\cdot) \leq 1$ function of the normalized time.

4.2.2. Around L_2

We design a very similar problem around L_2 .

Problem Statement. Consider two points $\chi_2^* \in \text{Het}$ and $\chi_3^* \in \text{Lya}_2$, a time t_2 and an initial mass m_2^* .³ The mass m_2^* is the final mass obtained after the solving for the transfer around L_1 (between the two problem we follow a heteroclinic orbit without any fuel consumption). We apply the Pontryagin Maximum Principle to the following problem:

$$\mathcal{P}_{L_2} \begin{cases} \min \int_0^{t_2} \|u\|^2 dt, \\ \dot{x} = F_0(x) + \frac{\epsilon}{m} \sum_{i=1}^2 u_i F_i(x), \\ \dot{m} = -\beta_* \epsilon |u|, \\ |u| \leq 1, \\ x(0) = \chi_2^*, m(0) = m_2^* \text{ and } x(t_2) = \chi_3^*. \end{cases} \quad (30)$$

³We will understand why we use 2 as subscript.

As before, we have fixed χ_2^* and χ_3^* on the heteroclinic and Lyapunov orbits. The final steps will allow us to release these constraints.

Since the problem is very similar to the problem around L_1 , we have the same hamiltonian and the same expression of the control u . Hence, we get the following shooting function:

$$\mathcal{S}_{L_2}(p(0), p_m(0)) = \begin{pmatrix} \phi_{1,\dots,4}^{\text{ext}}(\chi_2^*, m_2^*, p(0), p_m(0)) - \chi_3^* \\ \phi_{10}^{\text{ext}}(\chi_2^*, m_2^*, p(0), p_m(0)) \end{pmatrix} = \begin{pmatrix} 0 \\ 0 \end{pmatrix}. \quad (31)$$

Construction of χ_2^* and χ_3^* . We construct the two points following the same method.

- (1) If we denote by $\chi_{\text{Het}}^{L_2}$ the last point of the heteroclinic orbit near the Lyapunov orbit, we find $\chi_{\text{Lya}_2} \in \text{Lya}_2$ minimizing the euclidian norm : $\chi_{\text{Lya}_2} = \arg \min_{\chi \in \text{Lya}_2} \|\chi_{\text{Het}}^{L_2} - \chi\|$.
- (2) Then, we propagate forward χ_{Lya_2} following the uncontrolled dynamics during a time t_{Lya_2} (smaller than the period of Lyapunov orbit) to get χ_3^* .
- (3) We propagate backward the $\chi_{\text{Het}}^{L_2}$ during a reasonable time $t_{\text{Het}}^{L_2}$ to get χ_2^* (small compared to the traveling time to reach the other extremity).

We define the transfer time t_2 in (23) as

$$t_2 = t_{\text{Lya}_2} + t_{\text{Het}}^{L_2}.$$

Final State Continuation. As before, we construct a family of problems \mathcal{P}_λ depending continuously on one parameter λ such that \mathcal{P}_0 is easy to solve and \mathcal{P}_1 corresponds to the targeted problem, that is to say (23).

First, let us define $\chi_{\text{Het}}^{\text{nat}}$ as the forward propagation of χ_{Het} following the uncontrolled dynamics during the time t_2 . Then we define the family of problems:

$$\mathcal{P}_{L_2}^\lambda \begin{cases} \min \int_0^{t_2} \|u\|^2 dt, \\ \dot{x} = F_0(x) + \frac{\epsilon}{m} \sum_{i=1}^2 u_i F_i(x), \\ \dot{m} = -\beta_* \epsilon |u|, \\ |u| \leq 1, \\ x(0) = \chi_2^*, \quad m(0) = m_2^*, \\ x(t_2) = (1 - \lambda)\chi_{\text{Het}}^{\text{nat}} + \lambda\chi_3^*. \end{cases} \quad (32)$$

Numerical Results. As before, we set $T_{\text{max}} = 60$ N, and we compute the continuation for the two times chosen as :

$$t_{\text{Het}}^{L_2} = 2.0, \quad t_{\text{Lya}_2} = 1.0.$$

Figure 11 shows the optimal control to realize the final transfer from the heteroclinic orbit to the Lyapunov one around L_2 . We see that, once again, we are far from the saturation of u .

This continuation gives us an initial costate that we will denote by p_2^* and p_m^{2*} in the remainder of this work.

Table 2 sums up all the parameters for the continuation computation. We observe that, because we are using indirect shooting methods, the computation is very fast even though it is performed on a simple desktop computer or on a single-board computer (the Raspberry Pi).

4.3. Multiple Shooting

Thanks to the results from previous sections, we have designed an admissible control to perform the transfer from a Lyapunov orbit around L_1 to a Lyapunov orbit around L_2 . We first reach a point on a heteroclinic orbit,

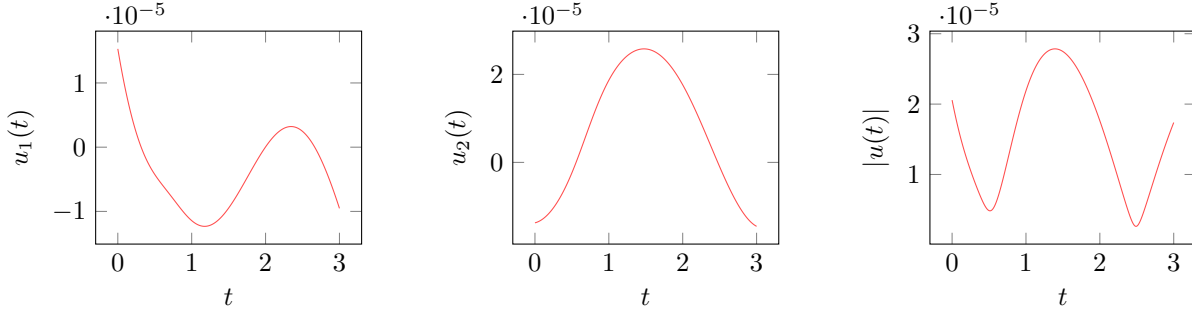


FIGURE 11. Command to realize the optimal transfer from the Lyapunov orbit to the heteroclinic orbit. We plot $u(\cdot) \leq 1$ as a function of the normalized time.

I_{sp}	g_0	Earth Mass	Moon Mass	Distance	Period
2000 s	$9.8 \text{ m}^3 \text{ kg}^{-1} \text{ s}^{-2}$	$5.972 \times 10^{24} \text{ kg}$	$7.349 \times 10^{22} \text{ kg}$	$384\,402 \times 10^3 \text{ m}$	$2.361 \times 10^6 \text{ s}$

Transfer	Iterations	Cost	T_{max}
L_1	21	$6.309\,67 \times 10^{-11}$	60 N
L_2	19	$9.061\,24 \times 10^{-10}$	60 N

System	Transfer	Execution time
Core i7	L_1	98% cpu 2,821s total
	L_2	96% cpu 1,439s total
Raspberry Pi A	L_1	38% cpu 8,009s total
	L_2	22% cpu 7,879s total

TABLE 2. Numerical results for the two transfers around L_1 and L_2 . Computations are made on a simple laptop Core i7, and on a Raspberry Pi A, a credit card-sized single-board computer.

then we follow the natural dynamics (null control), and finally reach a point on the final Lyapunov orbit from a certain point on the heteroclinic orbit.

These two points on the heteroclinic orbit are arbitrarily chosen. There is no guarantee that this a good choice in terms of optimality. Hence, we want to release these constraints on the position of these two points. We use a multiple shooting method on top of the first two local transfer to get a better optimum.

Let us describe how we state the multiple shooting problem. As we can see in figure 12, there are two points χ_1^* and χ_2^* belonging to the heteroclinic orbit that we want to free. Moreover, we have three times:

- t_0 which is the time defined for the transfer around L_1 ;
- t_2 which is the time defined for the transfer around L_2 ;
- t_1 which is the total time of the computed heteroclinic orbit minus the two times $t_{\text{Het}}^{L_1}$ and $t_{\text{Het}}^{L_2}$ used in the two previous transfers.

We define $t_{\text{tot}} = t_0 + t_1 + t_2$ and we write a new optimal control problem with the same structure as the previous one around L_1 and L_2 .

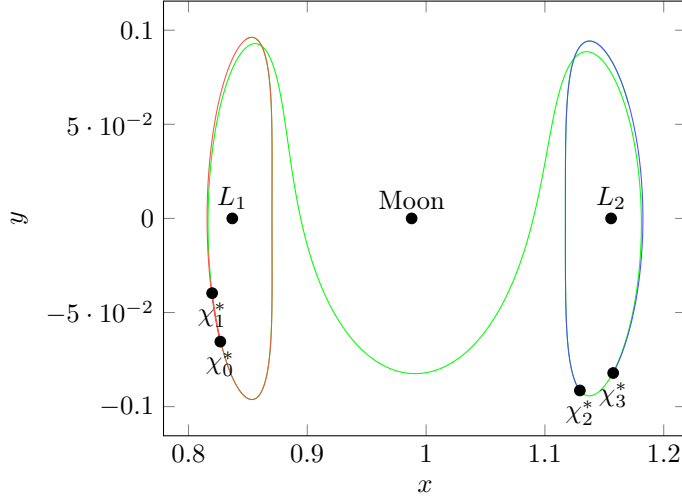


FIGURE 12. Admissible trajectory in three parts.

$$\mathcal{P}_{\text{tot}} \begin{cases} \mathcal{C}_{\text{tot}} = \min \int_0^{t_{\text{tot}}} \|u\|^2 dt, \\ \dot{x} = F_0(x) + \frac{\epsilon}{m} \sum_{i=1}^2 u_i F_i(x), \\ \dot{m} = -\beta_* \epsilon |u|, \\ |u| \leq 1, \\ x(0) = \chi_0^* \in \text{Lya}_1, \quad m(0) = m_0^*, \\ x(t_{\text{tot}}) = \chi_3^* \in \text{Lya}_2. \end{cases} \quad (33)$$

As before, we apply the Pontryagin Maximum Principle to get a necessary condition for the optimal control. We are able to write the control u depending on the state (x, m) and the costate (p, p_m) , we can write a shooting function, exactly with the results obtained in section 4.2. But because the system is very unstable, the initialisation of $p(0)$ from the transfer around L_1 is not good enough to make a single shooting method converge for the total transfer.

Thanks to the following method, we get an admissible trajectory in three parts, and it is quite natural to use it to construct a multiple shooting function. We define

$$Z = (\underbrace{p_0, p_m^0}_{P_0}, \underbrace{\chi_1, m_1}_{X_1}, \underbrace{p_1, p_m^1}_{P_1}, \underbrace{\chi_2, m_2}_{X_2}, \underbrace{p_2, p_m^2}_{P_2}) \in \mathbb{R}^{25},$$

then we write the multiple shooting function with two matching conditions on state and costate, the final state condition, and the free final mass:

$$\mathcal{S}_{\text{multi}}(Z) = \begin{pmatrix} \phi_{1,\dots,5}^{\text{ext}}(\chi_0^*, m_0^*, P_0) - X_1 \\ \phi_{6,\dots,10}^{\text{ext}}(\chi_0^*, m_0^*, P_0) - P_1 \\ \phi_{1,\dots,5}^{\text{ext}}(X_1, P_1) - X_2 \\ \phi_{6,\dots,10}^{\text{ext}}(X_1, P_1) - P_2 \\ \phi_{1,\dots,4}^{\text{ext}}(X_2, P_2) - \chi_3^* \\ \phi_{10}^{\text{ext}}(X_2, P_2) \end{pmatrix}. \quad (34)$$

We want to find the vector Z such that $\mathcal{S}_{\text{multi}}(Z) = 0$, and as in previous sections, we use a Newton-like algorithm. The main difficulty is as usual to initialize the algorithm. This time, it is done by the previous *local* transfers, indeed we chose:

$$\begin{cases} p_0 = p_0^*, \\ p_m^0 = p_m^{0*}, \\ \chi_1 = \chi_1^*, \\ m_1 = m_2^*, \\ p_1 = \underline{0}, \\ p_m^1 = 0, \\ \chi_2 = \chi_2^*, \\ m_2 = m_2^*, \\ p_2 = p_2^*, \\ p_m^2 = p_m^{2*}. \end{cases} \quad (35)$$

The choices $m_1 = m_2^*$, $p_1 = \underline{0}$ and $p_m^1 = 0$ are made because we initialize the trajectory with a heteroclinic part, that is to say with a null control and without consumption of mass.

The Newton-like algorithm gives us a complete trajectory which is not constrained to follow the heteroclinic orbit. In figure 14 and figure 13, we can see the trajectory and the associated command.

We keep the maximum thrust equal to 60 N to allow the Newton-like algorithm to converge. But, we want to be able to give the right specification for the engine of the spacecraft. Let us see how we make this possible.

4.4. Thrust Continuation

Following the continuation method we want to constrain the thrust to a real value for a low-thrust engine, let us say 0.3 N. To do that, we construct a family of problems as before. Let's denote by ϵ_0 the initial maximal thrust in normalized units corresponding to $T_{\text{max}} = 60$ N. Similarly, let us denote by ϵ_1 the maximal thrust that we want to get corresponding to $T_{\text{max}} = 0.3$ N. Finally, we define the maximal continuation thrust:

$$\epsilon_\lambda = (1 - \lambda)\epsilon_0 + \lambda\epsilon_1.$$

We can now define the family of problems:

$$\mathcal{P}_{\text{thrust}}^\lambda \begin{cases} \min \int_0^{t_{\text{tot}}} \|u\|^2 dt, \\ \dot{x} = F_0(x) + \frac{\epsilon_\lambda}{m} \sum_{i=1}^2 u_i F_i(x), \\ \dot{m} = -\beta_* \epsilon_\lambda |u|, \\ |u| \leq 1, \\ x(0) = \chi_0^* \in \text{Lya}_1, \quad m(0) = m_0^*, \\ x(t_{\text{tot}}) = \chi_3^* \in \text{Lya}_2. \end{cases} \quad (36)$$

We solve each step of the continuation with the previously defined multiple shooting method (34). This way, we manage to constrain the thrust to the given engine value. Since the control is smaller than 0.3 N, this continuation is easy, and the command does not change during it. In section 4.6 we summarize the numerical results.

Let us remark that the continuation is done with 22 iterations.

4.5. Optimization of the Terminal Points

The last remaining step is to free the initial and final points. The only constraints are that $x(0)$ has to belong to Lya_1 and $x(t_{\text{tot}})$ to Lya_2 . To simplify the problem, we have fixed by construction two points χ_0^* on Lya_1 and χ_3^* on Lya_2 . Now we want to find the optimal points on these two periodic orbits. So we want to solve the very

general problem (14). The Pontryagin Maximum Principle gives us two transversality conditions that we have to satisfy:

$$p_{1,\dots,4}(0) \perp T_{x(0)}\text{Lya}_1 \quad \text{and} \quad p_{1,\dots,4}(0) \perp T_{x(t_{\text{tot}})}\text{Lya}_2, \quad (37)$$

where the notation $T_x M$ stands for the usual tangent space to M at the point x (these conditions can be written as soon as the tangent space is well defined).

To perform this optimization we consider the two previously chosen points $\chi_0^* \in \text{Lya}_1$ and $\chi_3^* \in \text{Lya}_2$. First we perturb the point around Lya_2 following the decrease of the transversality condition until we find a good zero for the transversality condition. Since we checked that the evolution of this transversality condition along the periodic orbit is not monotone, we are just able to reach a local minimum. By doing this we manage to reach a transversality condition at t_{tot} around 1×10^{-8} . Secondly, we realize the same perturbation along Lya_1 and we manage to reach a value around 1×10^{-8} . We have checked that the inverse process beginning with the point on Lya_1 gives the same result.

Whereas this seems to be a very little change for the transfer (see numerical results in the next section), the structure of the obtained control is completely different from the previous command. We will describe this result deeper in the next section.

Remark: To perform this optimization, we could use a gradient method on the one-dimensional periodic orbits initializing it with the solution of the problem 36.

4.6. Numerical Results

Recall that we use the CRTBP parameters given in table 2. We see on figure 13 that the last optimization step change the shape of the control. Indeed, by construction, we make the spacecraft go onto the heteroclinic orbit before we free that constraint. Hence, it can be expected that the mission has *turnpike properties* (see [28]). That is to say the optimal solution settled in large time consists approximately of three pieces, the first and the last of which being transient short-time arcs, and the middle piece being a long-time arc staying exponentially close to the optimal steady-state solution. In figure 13, we see that before we satisfy the transversality conditions by the last optimization step, the command structure does not have the shape of a turnpike command. Control is spread along the trajectory. After the last optimization step, the control is clearly a turnpike control and the trajectory consists approximately in three pieces as expected.

We see on figure 14 the two corresponding trajectories. We can see that to reach to transversality conditions corresponding to $x(0) \in \text{Lya}_1$ and $x(t_{\text{tot}}) \in \text{Lya}_2$ we do not have to move the two fixed points very much. Cost. In this problem we are minimizing the cost:

$$\int_0^{t_{\text{tot}}} \|u\|^2 dt.$$

But we consider a mass evolving dynamical system, and a maximum thrust. To try to compare our obtained cost with other results as, we define three different costs:

$$\mathcal{C}_{\text{tot}}^1 = \int_0^{t_{\text{tot}}} \|u(t)\|^2 dt, \quad \mathcal{C}_{\text{tot}}^2 = \int_0^{t_{\text{tot}}} \frac{\epsilon^2}{m^2(t)} \|u(t)\|^2 dt, \quad \text{and} \quad \mathcal{C}_{\text{tot}}^3 = \int_0^{t_{\text{tot}}} \frac{T_{\text{max}}^2}{m^2(t)} \|u(t)\|^2 dt. \quad (38)$$

Results are summarized in table 3. We observe that whereas the two points χ_0^* and χ_3^* are not perturbed very much to satisfy the general transversality conditions, for the costs and the mass consumption, it is really an improvement.

5. VARIANT OF THE MISSION: HETEROCLINIC ORBIT WITH TWO REVOLUTIONS

In this section we present another mission going from a Lyapunov orbit around L_1 to a Lyapunov orbit around L_2 . We follow exactly the same method that we have presented here except that we first find the second

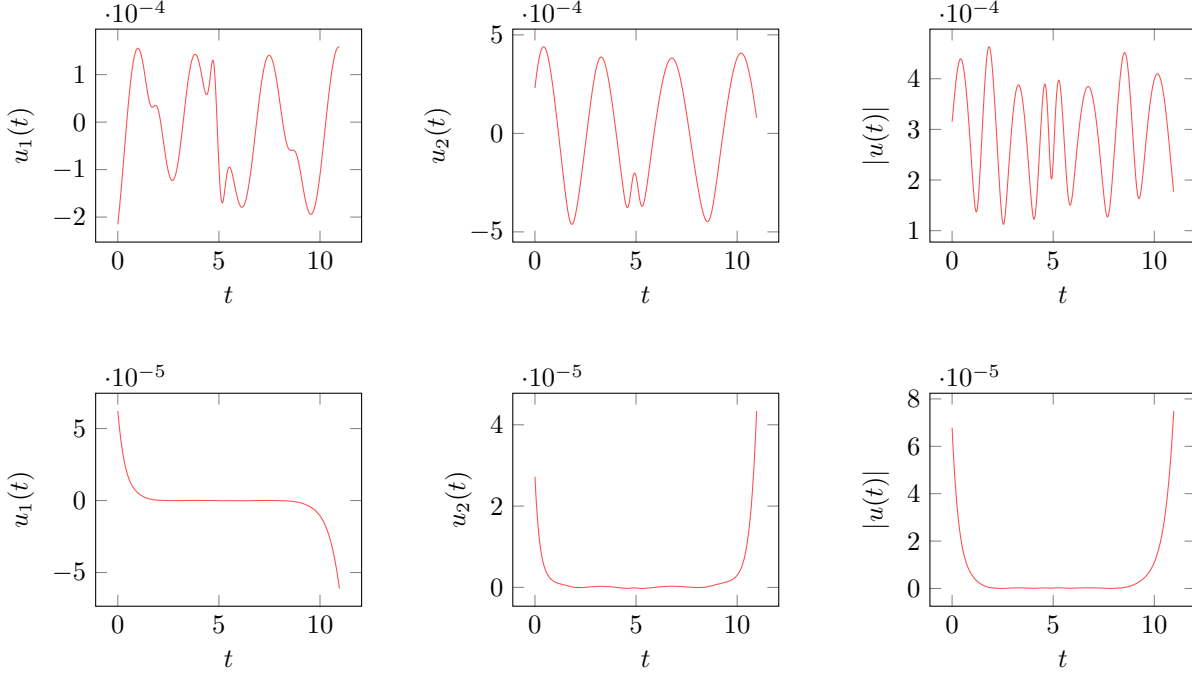


FIGURE 13. Command to realize the optimal transfer from the Lyapunov orbit to the heteroclinic orbit. We trace $u(\cdot) \leq 1$ before the last optimization step on the first row (we chose two points on Lya_1 and Lya_2) and after the last optimization step consisting in getting the general transversality conditions (second row). We can observe the good turnpike property of the second control.

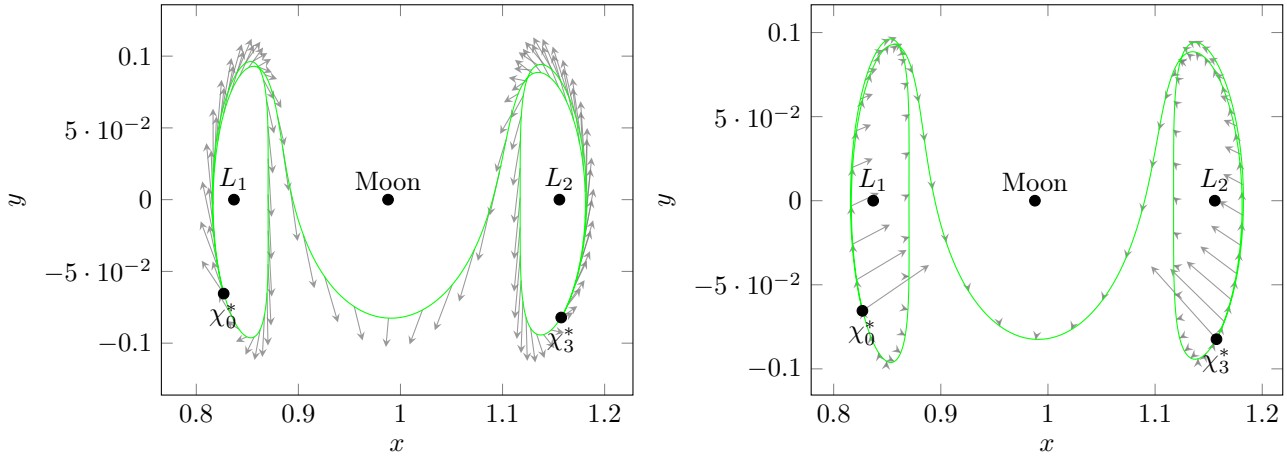


FIGURE 14. Optimal trajectory. On the left the optimal trajectory with χ_0^* and χ_3^* fixed on Lya_1 and Lya_2 . On the right, the optimal trajectory with χ_0^* and χ_3^* free on Lya_1 and Lya_2 .

intersection of manifolds, we compute the second crossing through the plane U_2 on both sides with the stable and unstable manifolds. Our final trajectory will perform two revolutions around the Moon.

	Initial Mass	Transfer time	T_{\max}
	1500 kg	10.961 39 or 47.67 days	0.3 N

	$\mathcal{C}_{\text{tot}}^1$	$\mathcal{C}_{\text{tot}}^2$	$\mathcal{C}_{\text{tot}}^3$	Mass of fuel
Problem (36)	$1.065\,018\,7 \times 10^{-6}$	$5.747\,987\,2 \times 10^{-9}$	$1.852\,784\,7 \times 10^{-13}$	0.018 687 8 kg
Problem (14)	$2.230\,596\,7 \times 10^{-9}$	$1.203\,855\,5 \times 10^{-11}$	$3.880\,463\,0 \times 10^{-16}$	$3.670\,958\,9 \times 10^{-4}$ kg

	System	Execution time
Problem (36)	Core i7	99% cpu 26,912s total
Problem (14)	Core i7	99% cpu 1min18,64s total
Problem (36)	Raspberry Pi A	20% cpu 15min3,545s total
Problem (14)	Raspberry Pi A	23% cpu 56min45,921s total

TABLE 3. Numerical results for the final trajectory of the first mission obtained after the multiple shooting with fixed departure and final points (problem (36)) and for the optimized departure and final points on Lya_1 and Lya_2 (problem (14)).

5.1. The Heteroclinic orbit

To compute the heteroclinic orbit with two revolutions around the Moon, we have to choose a certain energy allowing the second intersection to exist. We have chosen the energy (we follow [8] for the hint of this choice):

$$\mathcal{E}_{\text{Lya}_{1,2}} = -1.5890.$$

We manage to compute the heteroclinic orbit plotted in figure 15. We see that we have two revolutions around the Moon.

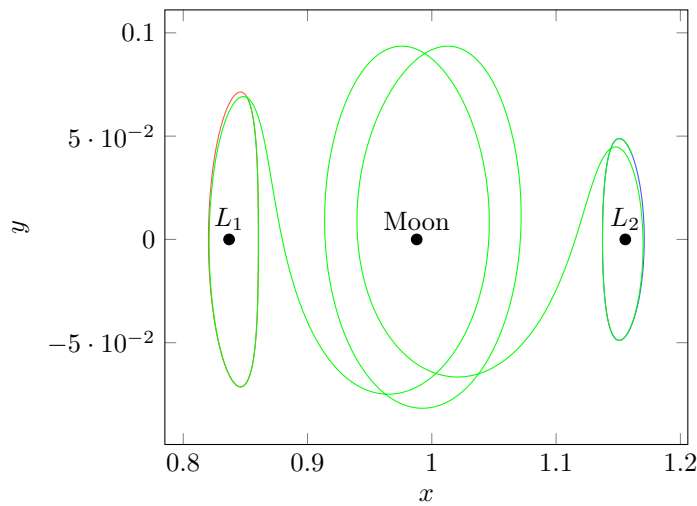


FIGURE 15. Heteroclinic orbit between two Lyapunov orbits in the Earth-Moon system. We get a travel time of 11.699681461946 (normalized time) or 50.883 days.

5.2. Two Local Transfers

As before, we compute two local transfers. One from the periodic orbit around L_1 to the heteroclinic orbit, and another from the end of the heteroclinic orbit to the periodic orbit around L_2 . We choose the maximal thrust equal to 60 N as before to help the success of the shoot. We do not report the partial results here as they are comparable to the ones of the previous mission. Thanks to this step, we obtain an admissible trajectory in three parts, one controlled to reach the heteroclinic orbit (the *turnpike*), the second part is the uncontrolled heteroclinic orbit, and the last part is a controlled one from the heteroclinic to the Lyapunov orbit around L_2 .

5.3. Multiple Shooting Method

As before, to free the two matching connections on the heteroclinic orbit and to decrease the maximum thrust we use a multiple shooting method associated with a continuation method. Since the transfer time is larger than for the previous mission, we have to add some grid points along the heteroclinic orbit (which are initialized with a null adjoint vector). This is due to the very unstable nature of this hamiltonian system. Here we chose 5 grid points. Thanks to the multiple shooting method and a thrust continuation, we manage to reach the required maximal thrust: $T_{\max} = 0.3$ N and we get an admissible trajectory with two fixed points on Lya_1 and Lya_2 . The last step consists in finding the optimal departure and arrival points on the two periodic orbits.

5.4. Optimization of the Terminal Points

Once again, because we have simplified the problem by fixing the departure and arrival points on Lya_1 and Lya_2 , we want to free these points on the periodic orbits to satisfy the general transversality conditions (37). As before, we perturb first $\chi_3^* \in \text{Lya}_2$ following the decrease of the transversality condition and we do the same with χ_0^* . We manage to satisfy the transversality conditions around 1×10^{-9} .

5.5. Results

We plot in figure 16 the command before and after the last optimization step. We observe the same phenomenon as for the previous mission. Indeed, before we satisfy the transversality conditions, the command does not have the *turnpike structure*, that is to say, the three parts, first a short thrust to reach the *highway*, then a null controlled part, and finally a controlled part to reach the periodic orbit.

Whereas the perturbations of the two points χ_0^* and χ_3^* to satisfy the transversality conditions are very small (see figure 17), the structure of the control is very different and the costs are much smaller after getting the transversality conditions. We summarize the numerical results in tables 4.

REFERENCES

- [1] Eugene L. Allgower and Kurt Georg. *Introduction to numerical continuation methods*, volume 45 of *Classics in Applied Mathematics*. Society for Industrial and Applied Mathematics (SIAM), Philadelphia, PA, 2003. Reprint of the 1990 edition [Springer-Verlag, Berlin; MR1059455 (92a:65165)].
- [2] Grégory Archambeau, Philippe Augros, and Emmanuel Trélat. Eight-shaped Lissajous orbits in the Earth-Moon system. *MathS in Action*, 4(1):1–23, 2011.
- [3] B. Bonnard, L. Faubourg, and E. Trélat. *Mécanique céleste et contrôle des véhicules spatiaux*, volume 51 of *Mathématiques & Applications (Berlin) [Mathematics & Applications]*. Springer-Verlag, Berlin, 2006.
- [4] J.-B. Caillau. *Contribution à l'étude du contrôle en temps minimal des transferts orbitaux*. Thèse de doctorat, Institut National Polytechnique de Toulouse, Toulouse, France, novembre 2000.
- [5] J.-B. Caillau and B. Daoud. Minimum time control of the restricted three-body problem. *SIAM J. Control Optim.*, 50(6):3178–3202, 2012.
- [6] O. Cots, J.-B. Caillau, and J. Gergaud. Hampath – A software for solving optimal control problems by indirect and path following methods (ADVANCED METHODS AND PERSPECTIVES IN NONLINEAR OPTIMIZATION AND CONTROL, Toulouse, 03/02/2010-05/02/2010). 2010.
- [7] B. Daoud. *Contribution au contrôle optimal du problème circulaire restreint des trois corps*. Thèse de doctorat, Université de Bourgogne, novembre 2011.

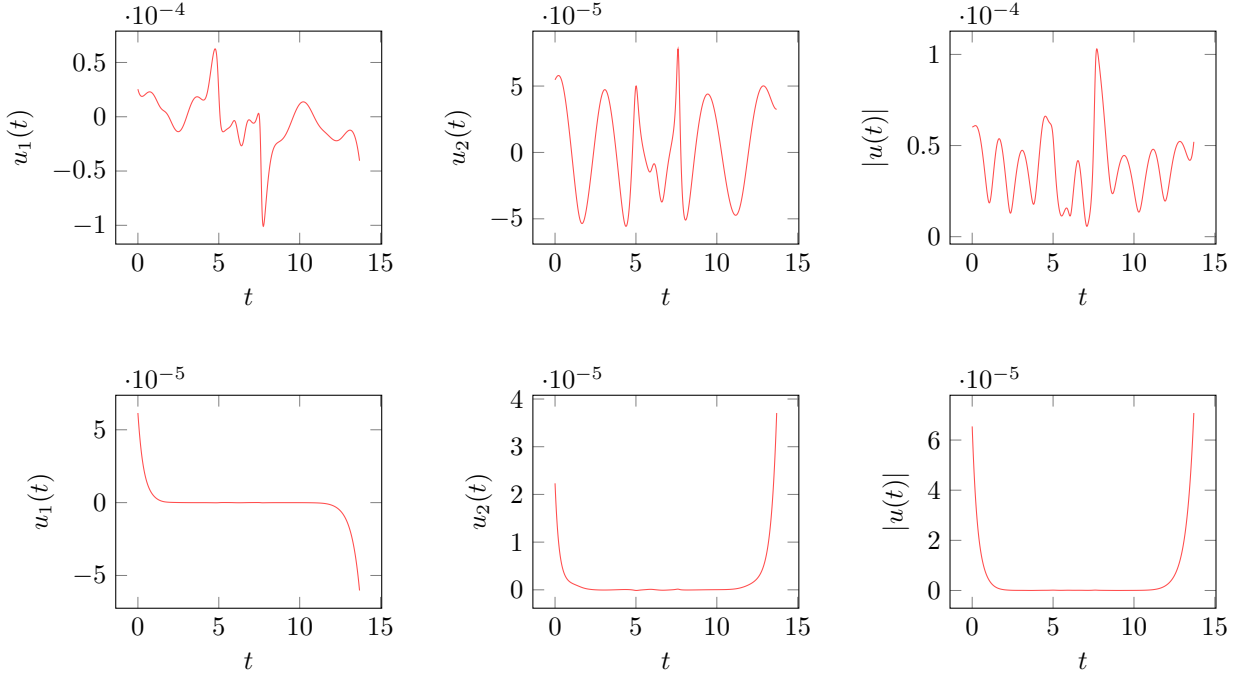


FIGURE 16. Command to realize the optimal transfer from the Lyapunov orbit to the heteroclinic orbit. We trace $u(\cdot) \leq 1$ before the last optimization step on the first row (we chose two points on Lya_1 and Lya_2) and after the last optimization step consisting in getting the general transversality conditions. We can observe the good turnpike property of the second control.

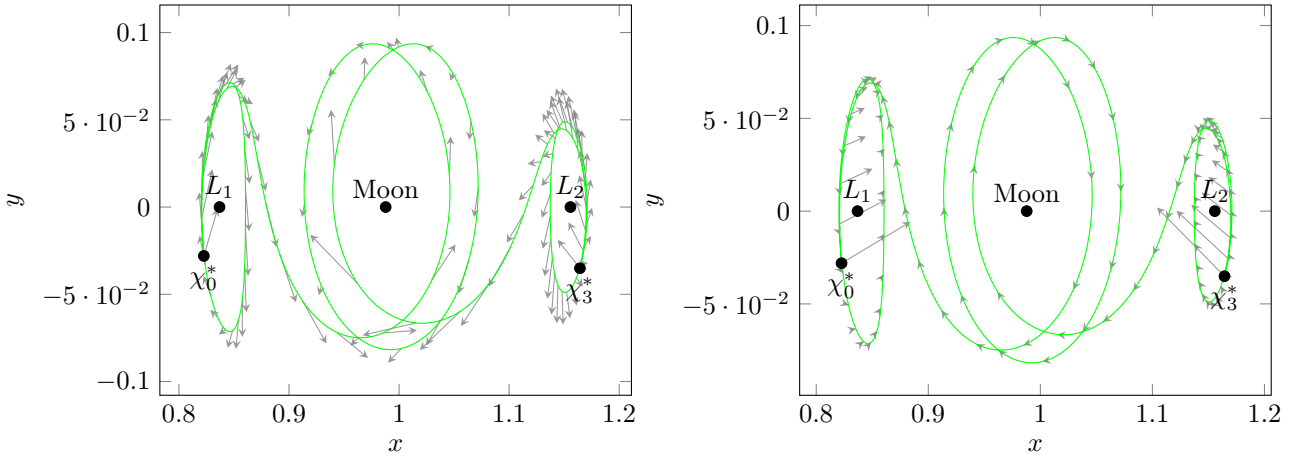


FIGURE 17. Optimal trajectory. On the left the optimal trajectory with χ_0^* and χ_3^* fixed on Lya_1 and Lya_2 . On the right, the optimal trajectory with χ_0^* and χ_3^* free on Lya_1 and Lya_2 .

- [8] R. Epenoy. Optimal long-duration low-thrust transfers between libration point orbits. In *Proceedings of the 63rd International Astronautical Congress*, volume 7, page 5670, Naples, Italy, 2012.
- [9] L. Euler. De motu rectilineo trium corporum se mutuo attrahentium. Oeuvres, Seria Secunda tome XXv Commentationes Astronomicae:144–151, 1767.

	Initial Mass	Transfer time	T_{\max}
	1500 kg	13.699 681 461 or 59.582 days	0.3 N

	$\mathcal{C}_{\text{tot}}^1$	$\mathcal{C}_{\text{tot}}^2$	$\mathcal{C}_{\text{tot}}^3$	Mass of fuel
Problem (36)	$2.463\,890\,5 \times 10^{-8}$	$1.329\,766\,7 \times 10^{-10}$	$4.286\,320\,4 \times 10^{-15}$	0.003 013 1 kg
Problem (14)	$1.969\,593\,4 \times 10^{-9}$	$1.062\,991\,7 \times 10^{-11}$	$3.426\,407\,9 \times 10^{-16}$	$3.359\,975\,0 \times 10^{-4}$ kg

	System	Execution time
Problem (36)	Core i7	99% cpu 44,949s total
Problem (14)	Core i7	99% cpu 2min54,79s total
Problem (36)	Raspberry Pi A	33% cpu 22min52,8s total
Problem (14)	Raspberry Pi A	29% cpu 1h32min46s total

TABLE 4. Numerical results for the final trajectory of the second mission obtained after the multiple shooting with fixed departure and final points (problem (36)) and for the optimized departure and final points on Lya_1 and Lya_2 (problem (14)).

- [10] R. W. Farquhar and A. A. Kamel. Quasi-periodic orbits about the translunar libration point. *Celestial mechanics*, 7(4):458–473, 1973.
- [11] R. W. Farquhar, D. P. Muhonen, C. R. Newman, and H. S. Heubergerg. Trajectories and Orbital Maneuvers for the First Libration-Point Satellite. *Journal of Guidance, Control, and Dynamics*, 3(6):549–554, 1980.
- [12] Joseph Gergaud and Thomas Haberkorn. Homotopy method for minimum consumption orbit transfer problem. *ESAIM Control Optim. Calc. Var.*, 12(2):294–310 (electronic), 2006.
- [13] G. Gomez and J. Masdemont. Some zero cost transfers between libration point orbits. In *POINT ORBITS, AAS PAPER 00-177, AAS/AIAA ASTRODYNAMICS SPECIALIST CONFERENCE*, 2000.
- [14] G. Gómez, J. Masdemont, and C. Simó. Lissajous orbits around halo orbits. *Adv. Astronaut. Sci.*, 1997.
- [15] G. Gómez, J. Masdemont, C. Simó, and A. Jorba. Study refinement of semi-analytical halo orbit theory: Executive summary. *ESOC Contract No.: 8625/89/D/MD (SC)*, 1991.
- [16] À. Jorba and J. Masdemont. Dynamics in the center manifold of the collinear points of the restricted three body problem. *Phys. D*, 132(1-2):189–213, 1999.
- [17] W. S. Koon, M. W. Lo, J. E. Marsden, and S. D. Ross. Dynamical systems, the three-body problem and space mission design. In *International Conference on Differential Equations, Vol. 1, 2 (Berlin, 1999)*, pages 1167–1181. World Sci. Publ., River Edge, NJ, 2000.
- [18] W. S. Koon, M. W. Lo, J. E. Marsden, and S. D. Ross. Heteroclinic connections between periodic orbits and resonance transitions in celestial mechanics. *Chaos*, 10(2):427–469, 2000.
- [19] J.-L. Lagrange. Essai sur le problème des trois corps. *Prix de l'académie royale des Sciences de paris, tome IX, Oeuvres de Lagrange* 6, Gauthier-Villars:272–282, 1772.
- [20] K. R. Meyer, G. R. Hall, and D. Offin. *Introduction to Hamiltonian dynamical systems and the N-body problem*, volume 90 of *Applied Mathematical Sciences*. Springer, New York, second edition, 2009.
- [21] G. Mingotti, F. Topputo, and F. Bernelli-Zazzera. Low-energy, low-thrust transfers to the moon. *Celestial Mechanics and Dynamical Astronomy*, 105(1-3):61–74, 2009.
- [22] G. Mingotti, F. Topputo, and F. Bernelli-Zazzera. Optimal low-thrust invariant manifold trajectories via attainable sets. *Journal of guidance, control, and dynamics*, 34:1644–1655, 2011.
- [23] L. S. Pontryagin, V. G. Boltyanskii, R. V. Gamkrelidze, and E. F. Mishchenko. *The mathematical theory of optimal processes*. Translated by D. E. Brown. A Pergamon Press Book. The Macmillan Co., New York, 1964.
- [24] D. L. Richardson. Analytic construction of periodic orbits about the collinear points. *Celestial Mech.*, 22(3):241–253, 1980.
- [25] Victor G. Szebehely. *Theory of Orbits - The Restricted Problem of Three Bodies*. Academic Press, 1967.
- [26] E. Trélat. *Contrôle optimal*. Mathématiques Concrètes. [Concrete Mathematics]. Vuibert, Paris, 2005. Théorie & applications. [Theory and applications].
- [27] E. Trélat. Optimal control and applications to aerospace: some results and challenges. *J. Optim. Theory Appl.*, 154(3):713–758, 2012.

- [28] E. Trélat and E. Zuazua. The turnpike property in finite-dimensional nonlinear optimal control. *J. Differential Equations*, 258(1):81–114, 2015.
- [29] L.T. Watson. *HOMPACK90: FORTRAN 90 Codes for Globally Convergent Homotopy Algorithms*. Department of Computer Science, Virginia Polytechnic Institute and State University, 1996.
- [30] F. B. Zazzera, F. Topputo, and M. Massari. Assessment of mission design including utilisation of libration points and weak stability boundaries. Technical Report 03-4103b, European Space Agency, the Advanced Concepts Team, 2004. Available online at www.esa.int/act.